

# Tower Based Load Measurements for Individual Pitch Control and Tower Damping of Wind Turbines

A A Kumar<sup>1</sup>, O Hugues-Salas<sup>2</sup>, B Savini<sup>2</sup> and W Keogh<sup>2</sup>

<sup>1</sup> Senior Control Engineer, DNV GL, Unit P, 101 Apollo Drive, Auckland, New Zealand

<sup>2</sup> DNV GL, One Linear Park, Avon Street, Temple Quay, Bristol, BS2 0PS, United Kingdom

E-mail: [avishek.kumar@dnvgl.com](mailto:avishek.kumar@dnvgl.com)

**Abstract.** The cost of IPC has hindered adoption outside of Europe despite significant loading advantages for large wind turbines. In this work we presented a method for applying individual pitch control (including for higher-harmonics) using tower-top strain gauge feedback instead of blade-root strain gauge feedback. Tower-top strain gauges offer hardware savings of approximately 50% in addition to the possibility of easier access for maintenance and installation and requiring a less specialised skill-set than that required for applying strain gauges to composite blade roots. A further advantage is the possibility of using the same tower-top sensor array for tower damping control. This method is made possible by including a second order IPC loop in addition to the tower damping loop to reduce the typically dominating 3P content in tower-top load measurements. High-fidelity *Bladed* simulations show that the resulting turbine spectral characteristics from tower-top feedback IPC and from the combination of tower-top IPC and damping loops largely match those of blade-root feedback IPC and nacelle-velocity feedback damping. Lifetime weighted fatigue analysis shows that the methods allows load reductions within 2.5% of traditional methods.

## 1. Introduction

A common feature of modern utility-scale wind turbines is the ability to use the blade pitch angle to dampen structural loading[1, 2].

Individual-pitch control (IPC) for wind turbines is a mature control feature applied to achieve reductions in asymmetric fatigue loading of turbine rotor/nacelle assemblies (RNA). Typical commercial implementations of IPC use blade-root based load sensing to provide feedback for IPC algorithms, however the additional cost of IPC has limited the majority of applications to the European OEM market in recent years [3]. The additional cost of IPC can be attributed to the cost of the sensors themselves, the cost of installation/maintenance of the sensors and the additional pitch activity required to perform IPC.

More common is the addition of tower damping through collective-pitch control (CPC). This feature reduces tower fatigue loading by modulating the collective blade pitch angle according to the velocity of the nacelle. Design standards dictate the necessity of a nacelle mounted acceleration signal for safety reasons[4], allowing the velocity signal to be recreated by integrating the acceleration signal.

In this work we investigate the use of a single tower-top-based load sensor array for both IPC and tower damping control loops. The tower-based sensors measure the tower tilting and yawing moments at the position applied. Tower-based strain gauges are in the order of 50%



the cost of blade-root based gauges, avoid potentially difficult access requirements to the blade roots, avoid the need for a specialised skill-set in applying gauges to composite blades and allow for a single sensor to apply both IPC and tower damping loops.

In Section 2 we summarise the typical IPC solution for wind turbines before presenting a methodology for applying IPC using tower based loading signals including a method for achieving higher-harmonic control; in Section 3 we discuss key features of tower damping loops before presenting the applicability of tower-top load based feedback for tower damping control loops, especially in the presence of IPC and finally in Section 4 we present results demonstrating the validity of the techniques outlined through both spectral and damage based metrics.

## 2. Individual Pitch Control

### 2.1. Background

Industry standard methods of implementing IPC for wind turbines use out-of-plane (OOP) blade-root moments to create individual pitch signals to reduce rotor asymmetric moments. The blade-root loads can be transformed into a non-rotating frame of reference using the Coleman transformation (effectively synonymous with the d-q axis transformation [1] and the multi-blade coordinate transformation [5]) to create three decoupled rotor loading signals: collective, cosine-cyclic and sine-cyclic:

$$\begin{bmatrix} M_{coli} \\ M_{cosi} \\ M_{sini} \end{bmatrix} = \begin{bmatrix} \frac{1}{3} & & \\ \frac{2}{3} \cos(i\psi) & \frac{2}{3} \cos(i(\psi + \frac{2\pi}{3})) & \frac{2}{3} \cos(i(\psi + \frac{4\pi}{3})) \\ \frac{2}{3} \sin(i\psi) & \frac{2}{3} \sin(i(\psi + \frac{2\pi}{3})) & \frac{2}{3} \sin(i(\psi + \frac{4\pi}{3})) \end{bmatrix} \begin{bmatrix} M_{y1} \\ M_{y2} \\ M_{y3} \end{bmatrix} \quad (1)$$

$$= T(\psi, i) \begin{bmatrix} M_{y1} \\ M_{y2} \\ M_{y3} \end{bmatrix} \quad (2)$$

where  $i$  is the transformation order;  $M_{coli}$  is the  $i^{\text{th}}$  order collective rotor load;  $M_{cosi}$  is the  $i^{\text{th}}$  order cosine-cyclic rotor load;  $M_{sini}$  is the  $i^{\text{th}}$  order sine-cyclic rotor load;  $\psi$  is the rotor azimuth angle; and  $M_{yx}$  is the OOP moment of the  $x^{\text{th}}$  blade.

If a first order transformation is applied, the resulting loads are very closely correlated with hub thrust, tilt and yaw loading respectively; higher order transformations are not quite so easily related to the physical system[6].

The asymmetric loading signals (cosine/sine-cyclic) are then fed back through separate IPC controllers to create cyclic pitch demands which can then be transformed back into the rotating frame to yield individual-pitch perturbations that are largely uncoupled from the collective-pitch actions of the generator speed controller and tower damper:

$$\begin{bmatrix} \Delta\theta_1 \\ \Delta\theta_2 \\ \Delta\theta_3 \end{bmatrix} = \sum_{i=1}^n T(\psi, i)^{-1} \begin{bmatrix} K_{cosi}(M_{cosi}) & 0 \\ 0 & K_{sini}(M_{sini}) \end{bmatrix} \quad (3)$$

where  $\Delta\theta_i$  is the blade pitch perturbation for blade  $i$ ,  $K_{cosi}$  is the controller for cosine-cyclic loads after an  $i^{\text{th}}$  order transformation; and  $K_{sini}$  is the controller for sine-cyclic loads after an  $i^{\text{th}}$  order transformation. For this work controllers  $K_{cosi}$  and  $K_{sini}$  are implemented as PI controllers.

Each transformation order essentially defines the rotor harmonic at which the pitch angle demands will modulate, for example first order transformations will demand pitch angle changes at 1P, and second order transformations will demand pitch angle changes at 2P and so forth. Pitch duty, rate and acceleration limits therefore usually restrict IPC implementations to first and second order transformations. Table 1 indicates the loading spectra targeted in rotating

components (e.g. blade) and non-rotating components (e.g. stationary hub) for the two orders of transformation.

Table 1: Targeted load frequencies

	Rotating	Non-rotating
1 <sup>st</sup> Order	1P	0P
2 <sup>nd</sup> Order	1P + 2P	0P + 3P

### 2.2. IPC with tower-based load measurements

As alluded to earlier, the first order transformations are very closely coupled to hub thrust, tilt and yaw loading; there is a slight difference due to rotor geometrical features such as rotor cone but these are minimal. The hub loading is in turn closely coupled to tower-top loading, with the latter containing additional moments due to the the RNA mass moment about the tower-top, the moment from thrust loading if the thrust vector is not aligned with the tower-top and any flexibility between the hub and tower-top. This relationship opens the possibility of replacing blade-root feedback with tower-top feedback in cases where the latter may be more cost-effective. Assuming a strain gauge measuring tilt and yaw on a tower with a centre-of-mass longitudinal offset  $o$  and vertical offset from the hub centre of  $v$ , the hub tilt and yaw loads (which closely approximate  $M_{\cos 1}$  and  $M_{\sin 1}$  respectively) can be estimated from the tower-based load measurements according to:

$$M_y = Q_y - (F_{\text{thrust}}v + F_{\text{mass}}o) \quad (4)$$

$$M_z = Q_z - Q_{\text{lss}} \sin(\theta_{\text{tilt}}) \quad (5)$$

where  $M_y$  is the estimated hub tilt moment,  $M_z$  is the estimated hub yaw moment,  $Q_y$  is the measured tower tilt moment,  $F_{\text{thrust}}$  is the rotor collective thrust load,  $F_{\text{mass}}$  is the RNA gravitational load,  $Q_z$  is the measured tower-yaw moment,  $Q_{\text{lss}}$  is the low-speed-shaft torque and  $\theta_{\text{tilt}}$  is the low-speed-shaft tilt angle.  $F_{\text{mass}}$ ,  $o$  and  $v$  are straight forward to derive from turbine models but determining  $Q_{\text{lss}}$  and  $F_{\text{thrust}}$  are less trivial. Assuming that the rotor aerodynamic torque is balanced by the demanded generator torque in above rated operation, we can posit an approximation of  $Q_{\text{lss}}$  according to:

$$Q_{\text{lss}} = Q_{\text{gen}}\mu \quad (6)$$

where  $Q_{\text{gen}}$  is the demanded generator torque and  $\mu$  is the gearbox ratio. The thrust load approximation can be made by solving the quasi-steady state thrust equation:

$$F_{\text{thrust}} = \frac{1}{2}\rho AC_t(V, \omega_r, \theta_{\text{col}})V^2 \quad (7)$$

where  $\rho$  is the air density,  $A$  is the rotor area,  $C_t$  is the coefficient of thrust,  $\omega_r$  is the rotor speed and  $V$  is the effective wind speed. A Luenberger wind-speed estimator based on that presented in [7] is used to recreate the wind speed and  $C_t$  is solved using a lookup table derived from a *Bladed* rotor-aerodynamic analysis. Clearly this method requires relatively accurate modeling of rotor aerodynamics and RNA mass moments, however both of these can be tuned to a prototype turbine where necessary. Errors in the thrust calculation are compounded the further the tower strain gauges are from the tower top, making this method most effective when strain gauges are mounted as high as possible.

### 2.3. Higher order IPC

It has been shown that the tower loads can be manipulated to reproduce hub loading, which represents a first order Coleman transformation. It is also possible to achieve higher order transformation by first transforming the tower loads to the rotating frame and then transforming them to the  $i^{\text{th}}$  order non-rotating frame as one would do with blade root loads.

$$\begin{bmatrix} 0 \\ M_{\cos i} \\ M_{\sin i} \end{bmatrix} = T(\psi, i)T(\psi, 1)^{-1} \begin{bmatrix} 0 \\ M_y \\ M_z \end{bmatrix} \quad (8)$$

In this process the collective component is assumed to be 0 as this component is not used for IPC in any case.

### 3. Tower Damping

Tower damping control loops dampen tower thrust loading caused by symmetric rotor loading as opposed IPC loops that target load reduction caused by asymmetric loading on the rotor. Symmetric rotor loading is most likely to excite the the turbine at the tower eigenfrequencies while asymmetric loading will generally excite the tower about the rotor harmonics. The closer to the tower-top the tower bending moments are measured, the higher the proportion of asymmetric loads that will be measured and vice versa. Ideally then, one would expect to measure tower loads as low on the tower as possible for most effective collective-pitch damping; this way pitch action is not wasted by reacting to asymmetric loads which are difficult to damp with modest collective-pitch demands. However, as a proxy for the tower-base load signal the nacelle fore-aft velocity signal can be used. This signal isolates collective loads, as collective loads have a significant impact on nacelle velocity. The signal also has the added bonus of having 0 low-frequency gain (otherwise the turbine would be moving away!), allowing the controller to ignore steady state loading on the tower. Incidentally, it is because of the 0 low-frequency gain that the nacelle acceleration/velocity feedback is difficult to use for IPC, as first order IPC specifically targets this low frequency load. The spectral characteristics of each discussed signal are illustrated in Figure 1. The relative positions of 1P (0.2 Hz), 3P and the first tower fore-aft frequency (0.33 Hz) can easily be seen in the Figure.

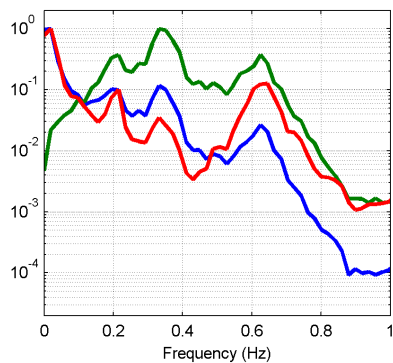


Figure 1: Normalised autospectra for tower-base tilt moment (blue), nacelle fore-aft velocity (green) and tower-top tilt moment (red).

We can see the impact of applying tower damping with tower-top feedback compared to nacelle-velocity feedback in Figure 2. The tower-base tilt moment autospectra shows the tower-top based tower-damping reduces the tower eigenfrequency peak, but not as deeply as with nacelle-velocity feedback. We also see a significant amount of pitching at 3P in both the time series and blade pitch autospectra.

The introduction of second order IPC transforms the playing field. Second order IPC suppresses 0P and 3P loading on the tower-top in the tilt direction, changing the relative

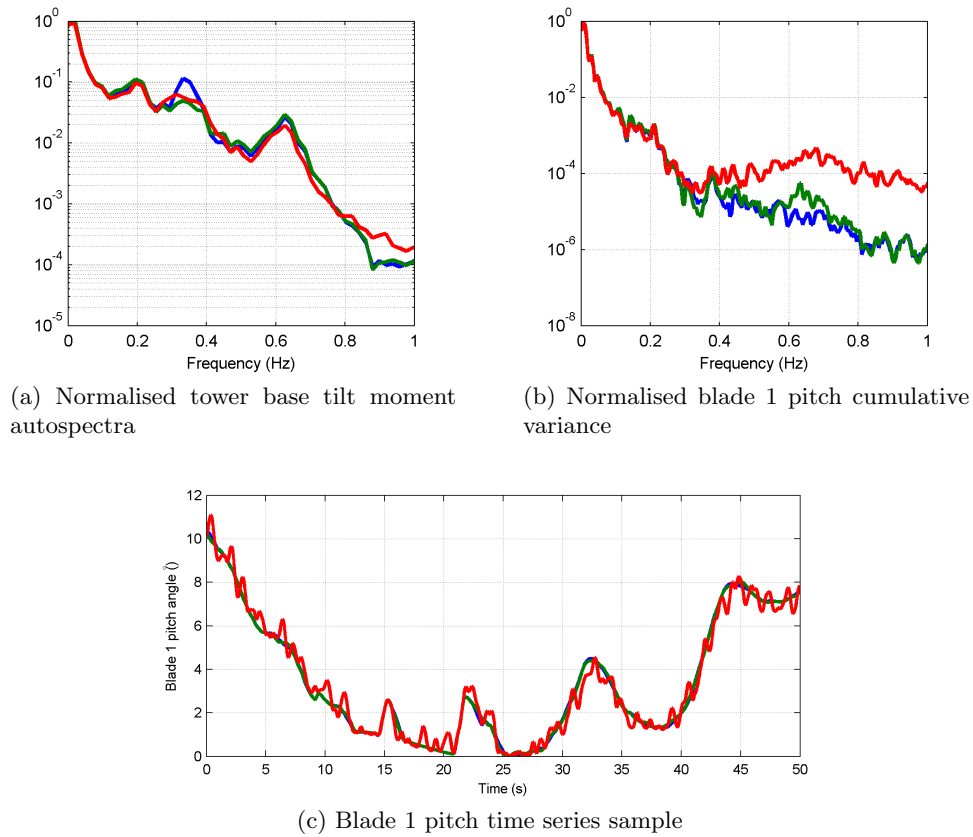


Figure 2: Tower damping response with no IPC in turbulent wind. No damping (blue), nacelle fore-aft velocity feedback (green), tower-top tilt moment feedback (red).

difference in 3P signals and tower eigenfrequency signals. Figure 3 shows the normalised tower spectra with second order tower-top feedback IPC active. We can see the tower-top tilt load spectra now has characteristics that are more similar to the tower-base tilt load spectra with the 3P response below that of the tower eigenfrequency response. This coupled by the attraction of being able to use a single sensor for both IPC and tower damping (and/or fault tolerance to sensor failure) has prompted further investigation.

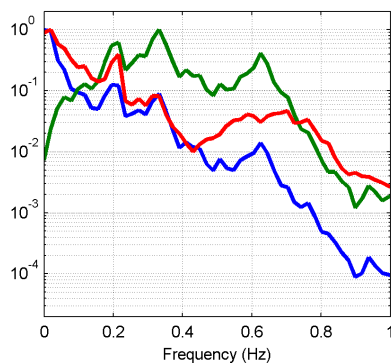


Figure 3: Normalised autospectra for tower-base tilt bending moments (blue), Nacelle fore-aft velocity (green) and tower-top tilt bending moments (red) with 2P tower-top IPC active.

## 4. Results and Discussion

### 4.1. Simulation environment

All comparisons conducted in this work are performed using a high-fidelity *Bladed* model of a 3 MW variable speed wind turbine with headline turbine parameters listed in Table 2. Wind conditions for simulations adhere to IEC 3rd Edition onshore wind turbine design standards for Class III A conditions[8]. The tower-based sensors are mounted 6.5 m below the tower-top to avoid the influence of tower stress gradients near the yaw bearing, and to avoid any sensor noise that may be exacerbated by the electrical system in the nacelle.

Table 2: Turbine model headline parameters

Rotor Diameter	Hub Height	Rated Rotor Speed
114 m	88 m	12.6 rpm

### 4.2. Recreation of hub loading

The ability to recreate the hub tilt and yaw moments from tower measurements is demonstrated through a 10-minute simulation in turbulent wind. Figures 6 and 7 show sample time series of the actual and estimated tilt and yaw loads. We see a much closer approximation of the yaw loading than the tilt loading, as the former does not require estimation of thrust related moments. A spectral comparison of the estimated and actual hub-tilt moments (Figure 4) shows a slight over-prediction of tilt loads between 1P and the tower first eigenfrequency. However, the IPC controller would be targeting 0P (steady) and 3P loads in the non-rotating frame, which show a much closer agreement than the aforementioned frequencies. A spectral comparison of the hub-yaw moments shows a very close agreement well beyond 3P.

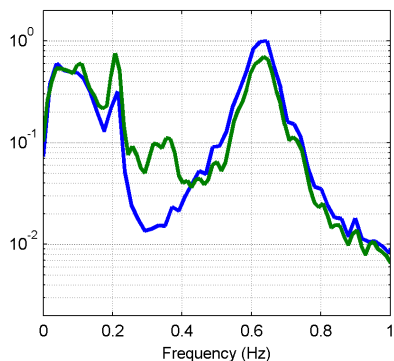


Figure 4: Normalised autospectra of actual (blue) and estimated (green) hub tilt loading in turbulent wind.

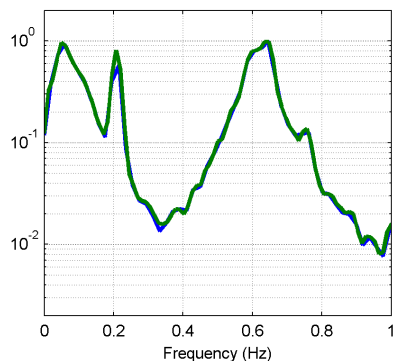


Figure 5: Normalised autospectra of actual (blue) and estimated (green) hub yaw loading in turbulent wind.

### 4.3. IPC performance

First and second order blade-root and tower-top based proportional-integral (PI) controllers have been tuned to give similar performance. To achieve this, a scale of  $\frac{2}{3}$  and an additional notch

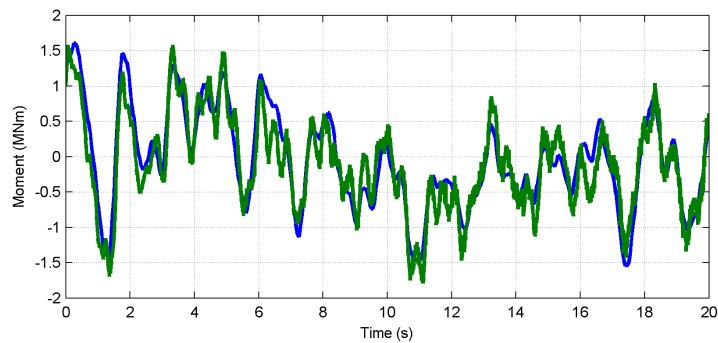


Figure 6: Time series sample of actual (blue) and estimated (green) hub tilt loading in turbulent wind.

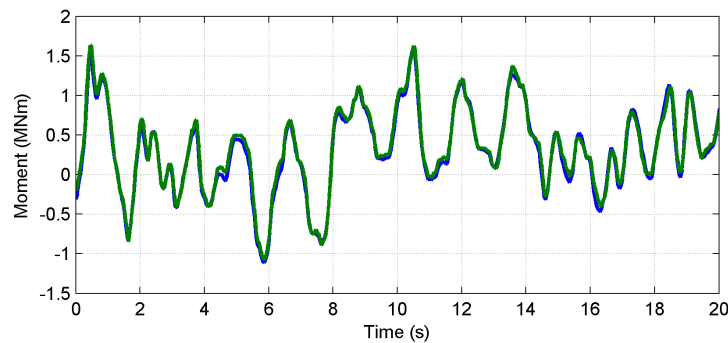


Figure 7: Time series sample of actual (blue) and estimated (green) hub yaw loading in turbulent wind.

filter at the tower eigenfrequency frequency is applied to the blade-root tuned controller for use with tower-top feedback. All controllers in this section also include a nacelle-acceleration based tower damper. Figures 8a through 8d show the spectral responses of a series of simulations for a collective pitch controller (CPC), first and second order blade-root-feedback IPC controllers (1P-blade-root IPC and 2P-blade-root IPC), and first and second order tower-top-feedback IPC controllers (1P-tower-top IPC and 2P-tower-top IPC). The spectra clearly show that tower-top feedback IPC achieved reductions at similar target frequencies to the blade-root feedback IPC for both first and second order transformations. Both first order controllers reduced 0P loads in the hub tilt and yaw directions, as well as reducing 1P loads in the blade-root OOP direction, while both second order controllers also reduced 3P loads in the hub tilt and yaw directions and 2P loads in the blade-root OOP direction. We can also see that the cumulative variance of the blade pitch angle is similar for both IPC controllers, with the first order tower-top feedback IPC controller using less pitch than the blade-root equivalent, and the second order using slightly more. The tower-top feedback controllers do show a slightly less spectral reduction in blade-root OOP loading at 1P relative to the blade-root based method. This is not surprising however as both controllers are targeting slightly different load sources: the hub tilt/yaw and the rotor tilt/yaw. The latter favours blade-root load reduction at 1P. It should be noted that the spectra shows the IPC controllers exacerbating 1P loads in the hub relative to CPC; 1P loads are dominated by imbalances (a blade offset imbalance was included in this model), which can be excited by using IPC. Solving this problem is outside the scope of this work, however effective methods exist including [9].

The second order controllers have been tested across a full range of IEC 3<sup>rd</sup> Edition normal

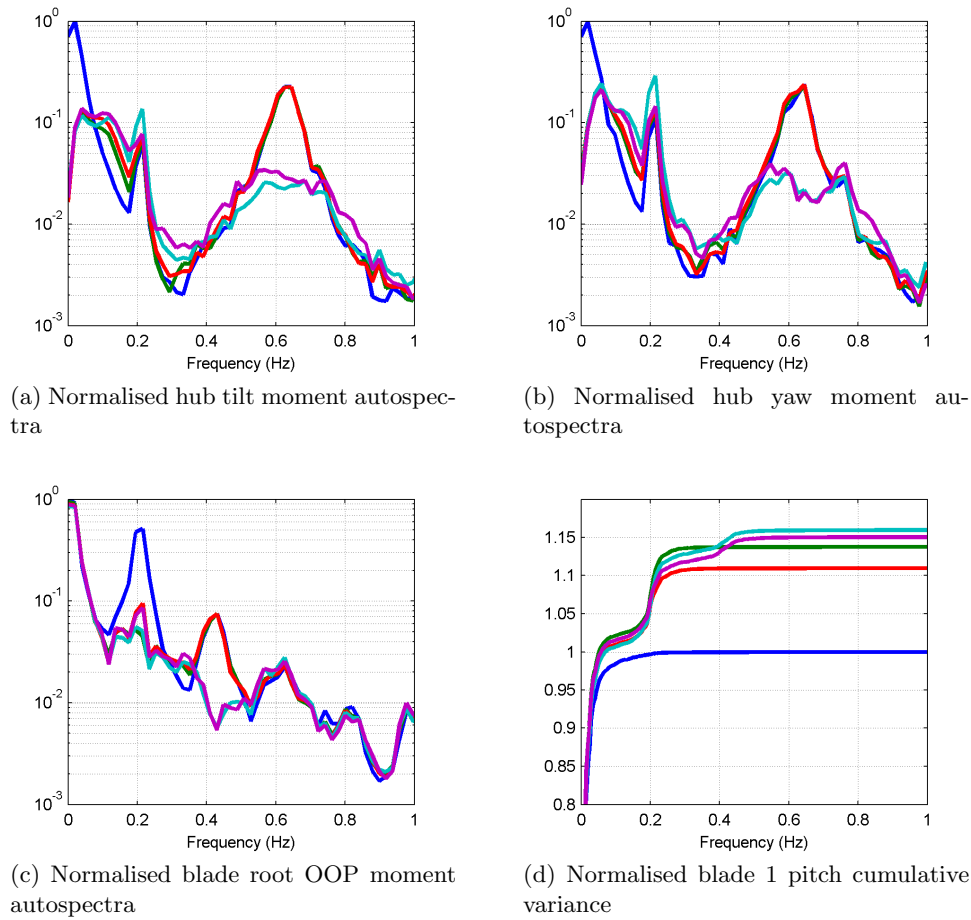


Figure 8: Spectral response in turbulent wind using CPC (blue), 1P-blade-root IPC (green), 1P-tower-top IPC (red), 2P-blade-root IPC (cyan) and 2P-tower-top IPC (magenta) in turbulent wind.

operation (Design Load Case 1.2) simulations to calculate an approximate lifetime weighted damage equivalent load (DEL). Each controller has been run with a total of 66 ten-minute simulations, from cut-in ( $3 \text{ m}\cdot\text{s}^{-1}$ ) to cut-out ( $24 \text{ m}\cdot\text{s}^{-1}$ ) wind speeds, and with three different wind inflow directions ( $-8^\circ$ ,  $0^\circ$ ,  $8^\circ$ ). Results for components of interest are given in Table 3. The results indicate very close load reduction levels for both IPC controllers across hub, blade and tower base fatigue loads relative to the CPC controller. The tower-top feedback controller shows reductions within 2% of the standard blade-root based method.

#### 4.4. Tower damping performance

A nacelle-velocity feedback damper and a tower-top moment feedback damper have been designed to show similar disturbance rejection to collective thrust inputs. Linear frequency responses and step responses from collective wind speed to tower-base tilt moment are given in Figure 9.

We saw in Figure 2 that the tower-top feedback damper introduced significant pitching above the tower eigenfrequency relative to the velocity-feedback tower damper. However when we introduce second order IPC, the relative pitch activity becomes very similar between the two

Table 3: Normalised lifetime DELs with second order IPC controllers (SN Slope = 3, 1 Hz Freq.)

Controller	Hub Tilt	Hub Yaw	Blade Root OOP	Tower Base Fore-Aft
CPC	100%	100%	100%	100%
2P-blade-root	85.5%	88.9%	80.3%	101.5%
2P-tower-top	86.4%	88.0%	81.6%	102.0%

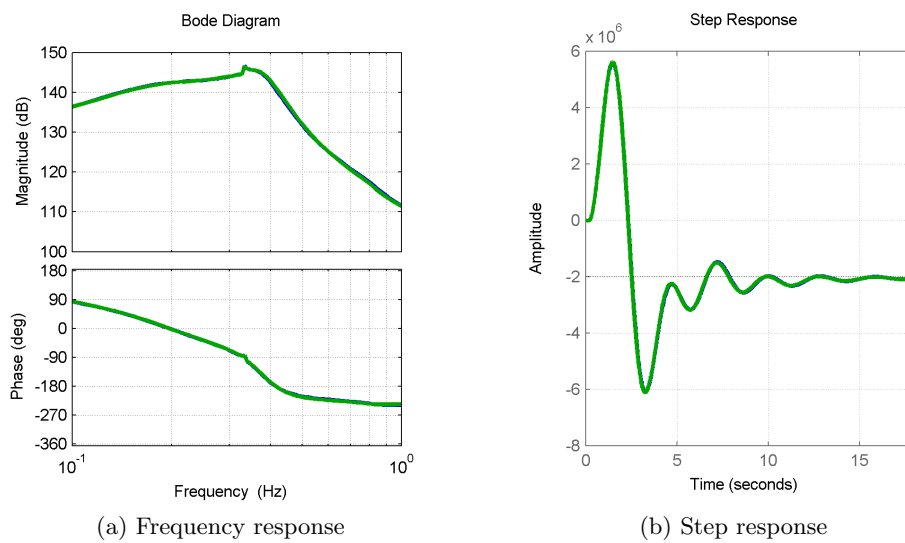


Figure 9: Linear response for nacelle-velocity feedback damping (blue), and tower-top load feedback (green).

as shown in Figure 10. This is attributable to the naturally increased high frequency pitching from using second order IPC, but also from the reduction in 3P loading on the tower that this IPC brings. Both controllers show a clear reduction of the spectral response around the tower eigenfrequency and at 3P. Interestingly, the tower-top feedback damper achieves lower 1P loading than the velocity-feedback damper.

The equal performance of both controllers is further validated across a full range of IEC 3<sup>rd</sup> Edition normal operation (Design Load Case 1.2) simulations (see Section 4.3). Results are summarised for key components in Table 4 and show very little variation (<2.5%) between 2P-blade-root IPC with velocity feedback tower damping and 2P-tower-top feedback IPC with tower-top moment damping.

## 5. Conclusions

The cost of IPC has hindered adoption outside of Europe despite significant loading advantages for large wind turbines. In this work we have presented a method for applying IPC (including for higher-harmonics) using tower-top strain gauges instead of blade-root strain gauges. These offer hardware savings of approximately 50% in addition to the possibility of easier access for maintenance and installation and requiring a less specialised skill-set than that required

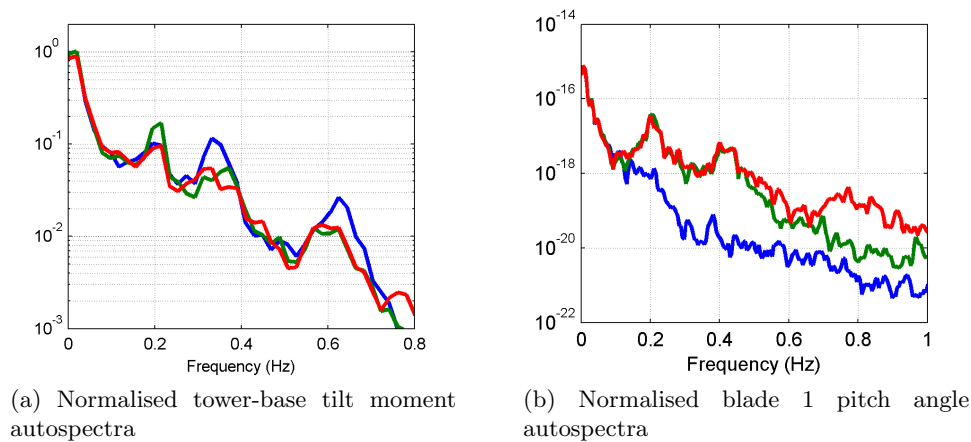


Figure 10: Spectral response of controller with no tower damping (blue), velocity-feedback damping and 2P-blade-root IPC (green) and tower-top moment feedback damping 2P IPC (red).

Table 4: Normalised lifetime DELs with second order IPC controllers and tower damping (SN Slope = 3, 1 Hz Freq.)

Controller	Hub Tilt	Hub Yaw	Blade Root OOP	Tower Base Fore-Aft
CPC + velocity feedback	100%	100%	100%	100%
2P-blade-root + velocity feedback	86.3%	89.2%	80.5%	100.8%
2P-tower-top + tower-top damping	88.5%	89.2%	82.5%	101.2%

for applying strain measurements to composite blade roots. High-fidelity *Bladed* simulations show that the resulting turbine spectral characteristics from tower-top feedback IPC largely match those of blade-root feedback IPC and lifetime weighted fatigue analysis shows that the method allows load reductions within 2% of traditional methods. A further advantage is the possibility of using the same tower-top sensor array for tower damping control. This method is made possible by including a second order IPC loop in addition to the tower damping loop. The combination of control loops reduces the typically dominating 3P content in tower load measurements. Simulations confirm that spectral characteristics match very closely with nacelle-velocity feedback damping and lifetime weighted fatigue loads are within 2.5% of traditional methods.

## References

- [1] Bossanyi E A 2003 *Wind Energy* **6** 119–128
- [2] Bossanyi E A 2003 *Wind Energy* **6** 229–244
- [3] Serrano-Gonzalez J and Lacal-Artegui R 2016 *Wind Energy (preprint)* URL <http://dx.doi.org/10.1002/we.1974>
- [4] 2016 DNVGL-ST-0438: Control and protection systems for wind turbines
- [5] Bir G 2008 *ASME Wind Energy Symp.*
- [6] van Engelen T G 2006 *EWEC March* (Athens, Greece)
- [7] Kumar A A, Bossanyi E, Scholbrock A K, Fleming P A and Boquet M 2015 *EWEA* (Paris)
- [8] IEC 2005 *IEC 61400-1 Wind turbines - Part 1: Design requirements* 3rd ed (Geneva: IEC)
- [9] Duckwitz D and Shan M 2012 *J. Phys.: Conf. Series* vol 555 (IOP Publishing)